BJRS
BRAZILIAN JOURNAL OF RADIATION SCIENCES

doi.org/10.15392/2319-0612.2026.2993
Braz. J. Radiat. Sci., Rio de Janeiro
2026, 14(1) | 01-21| e2993
Editor: Prof. Dr. Bernardo Maranhão Dantas
Editor: Prof. Dr. Alfredo Lopes Ferreira Filho
Submitted: 2024-08-04
Accepted: 2025-12-03

Original Article

Application of Feedforward Neural Networks for Virtual Sensor Implementation in Nuclear Reactors

Wu[a*], F.E.; Conti[a], T. N.

[a] Nuclear and Energy Research Institute, 05508-000, São Paulo, SP, Brazil.

*Correspondence: fred.wu@alumni.usp.br

Abstract: This study builds on a line of research developed at the Nuclear and Energy Research Institute (IPEN), focused on the use of Artificial Neural Networks (ANNs) to provide sensor redundancy in nuclear reactors. The proposed methodology consists of training a Feedforward Neural Network (FFNN) to estimate the value of one reactor variable based on measurements from other variables. The feasibility was demonstrated using data from IPEN's nuclear research reactor and a scaled model. While previous works relied on data from a single operating cycle of the reactor, this study tested network performance using data from multiple cycles to assess accuracy and generalization, and to identify deficiencies in the method. One fault-free cycle was selected for training and validation, while five others were used for testing, featuring different events. Three temperature variables, three radiation variables, one power measurement, and one safety rod position were chosen as output sensors for the ANNs to estimate. Performance was evaluated using the Mean Absolute Percentage Error (MAPE). All ANNs performed well during training. However, only two temperature variables were estimated across all the test cycles with similar accuracy as in the training and validation process, with MAPE values below 3%. Other ANNs performed poorly, with instances of persistent offsets or failure to track the general shape of the measured signals. The results underscore the challenges posed by strong input-output correlations and the difficulty in capturing the full complexity of functional relationships within reactor variables.

Keywords: nuclear reactor, sensor redundancy, sensor failure, artificial neural network.

SBPR

doi.org/10.15392/2319-0612.2026.2993
Braz. J. Radiat. Sci., Rio de Janeiro
2026, 14(1) | 01-21| e2993
Editor: Prof. Dr. Bernardo Maranhão Dantas
Editor: Prof. Dr. Alfredo Lopes Ferreira Filho
Submitted: 2024-08-04
Accepted: 2025-12-03

Aplicação de Redes Neurais Feedforward na implementação de Sensores Virtuais em Reatores Nucleares

Resumo: Este estudo dá continuidade a uma linha de pesquisa desenvolvida no Instituto de Pesquisas Energéticas e Nucleares (IPEN), focada no uso de Redes Neurais Artificiais (RNAs) para alcançar redundância de sensores em reatores nucleares. A metodologia proposta consiste em treinar uma *Rede Neural Feedforward* (FFNN) para estimar o valor de uma variável do reator com base em medições de outras variáveis. A viabilidade foi demonstrada utilizando dados do reator nuclear de pesquisa do IPEN e um modelo em escala. Enquanto trabalhos anteriores se basearam em dados de um único ciclo operacional do reator, este estudo avaliou o desempenho das redes utilizando dados de múltiplos ciclos com o objetivo de verificar a precisão, a generalização, e identificar deficiências no método. Um ciclo livre de falhas foi selecionado para treinamento e validação, enquanto outros cinco foram usados para testes, abrangendo diferentes eventos. Três variáveis de temperatura, três de radiação, uma medição de potência e a posição de uma barra de segurança foram escolhidas para as redes estimarem. O desempenho foi avaliado por meio do *Mean Absolute Percentage Error* (MAPE). Todas as redes apresentaram bons resultados durante o treinamento. No entanto, apenas as redes de duas variáveis de temperatura obtiveram precisão similar nos ciclos de teste, apresentando valores de MAPE abaixo de 3%. As demais tiveram desempenho insatisfatório, com casos de desvios persistentes ou falha em acompanhar a tendência geral dos sinais medidos. Os resultados destacam os desafios impostos por correlações fortes entre entradas e saídas, bem como a dificuldade em capturar toda a complexidade das relações funcionais entre as variáveis do reator.

Palavras-chave: reator nuclear, redundância sensorial, falha sensorial, rede neural artificial.

1. INTRODUCTION

Redundancy is crucial for ensuring the safety of nuclear reactors. Components and systems such as pumps, batteries, and emergency cooling mechanisms typically have backups - and so do sensors. In early reactor designs, only physical redundancy was possible, meaning the deployment of multiple sensors to measure the same variable. However, with advances in computational techniques, analytical redundancy has become feasible, offering prospects for reducing maintenance costs and operational complexity in nuclear power plants. In this context, Artificial Intelligence (AI) and machine learning algorithms can help overcome the challenges of analytical modeling complex systems and to extract meaningful information directly from data.

Numerous AI applications in nuclear systems have been proposed. BARTLETT and UHRIG (1992) demonstrated early diagnosis of nuclear reactor accidents using multilayer perceptron (MLP) networks, optimizing the number of nodes and using reactor sensor data as input. Similarly, GOMES and MEDEIROS (2015) employed radial basis function (RBF) networks for the same purpose with successful outcomes. YUE *et al.* (2020) developed an Artificial Neural Network (ANN) using meteorological and gamma dose rate data to predict the category of radioactive release in accident scenarios. Their approach included optimization of network weights using Genetic Algorithms (GA) and Simulated Annealing (SA), followed by training and the reconstruction of missing dose data via Particle Swarm Optimization (PSO). SAEED and RASHID (2020) designed an ANN to map reactor core power distribution from operational data, achieving rapid and accurate estimations.

Considerable research has also been dedicated to the simulation of sensor readings. NABESHIMA *et al.* (1998, 2002) proposed a method in which an ANN uses all available sensor readings to estimate subsequent values, including a retraining algorithm that adapts the network to evolving reactor conditions. Their system was capable of identifying sensor

malfunctions and, when combined with an expert system, diagnosing valve failures and leaks. MESSAI *et al.* (2015) modeled the reading of a temperature sensor using control rod positions and coolant flow as inputs to an ANN. MANDAL (2015) successfully trained an ANN with 181 inputs and outputs to model sensor data from a Fast Breeder Test Reactor. Convolutional Neural Networks (CNNs) were explored by LEE *et al.* (2021), who represented reactor state values as two-dimensional images and temporal differences as additional input channels. This method allowed the network to extract information from time-varying behavior in reactor variables. By adjusting the time window between states, the authors evaluated its impact on classification performance across 10 event types over 3300 scenarios lasting 30 seconds—yielding promising results. An alternative approach was proposed by DENG and HOOI (2021), who, although working with water treatment data, adapted Graph Neural Networks (GNNs) to model individual sensors as nodes and their interrelationships as edges, showing potential for application in nuclear monitoring. Furthermore, CAIXETA *et al.* (2025) highlights the importance of feature importance and outlier detection in a study featuring different types of deep neural networks as virtual sensor alternatives for Mobile Temperature Sensors (MTSs) at the Angra I Nuclear Power Plant. The use of Feature Importance methods improved performance, with the CNN, for instance, going from a Mean Absolute Error (MAE) of 3.194 using Principal Component Analysis (PCA) to 0.592 with XGBoost/Random Forest, further improved to 0.497 using Density-Based Spatial Clustering of Applications with Noise (DBSCAN) for outlier detection.

At IPEN, several studies have been conducted to evaluate the use of training Feedforward Neural Networks (FFNN) as virtual sensors for reactor variables. Here, the proposed method is to use readings from a subset of variables as input for a network trained to estimate the values of another, specified, variable in real time. BUENO (2011) trained and validated networks using data from both simulation models of the Institute of Atomic Energy-Reactor One (IEA-R1) research reactor and one of its operating cycles, estimating values for a large set of sensors. Each sensor was modeled by a dedicated ANN using other sensor readings as input. The Group Method of Data Handling (GMDH) was employed to

select the most relevant input variables for each case. Later, SANTOS (2016) introduced ant colony optimization (ACO) to optimize the internal structure of the networks, yielding hidden layers with fewer neurons and recurrent connections. Further validation was conducted by MORAES (2019) using a small-scale experimental replica of the reactor. The work presented here expands upon this line of research.

1.1. The IEA-R1 research reactor

Reaching criticality in 1957, the IEA-R1 is the first nuclear reactor built in Brazil. It is a 5 MW open pool research reactor, with a schematic presented in Figure 1:

Figure 1: IEA-R1 research reactor schematic. Primary and secondary cooling loops are shown with key components labeled.

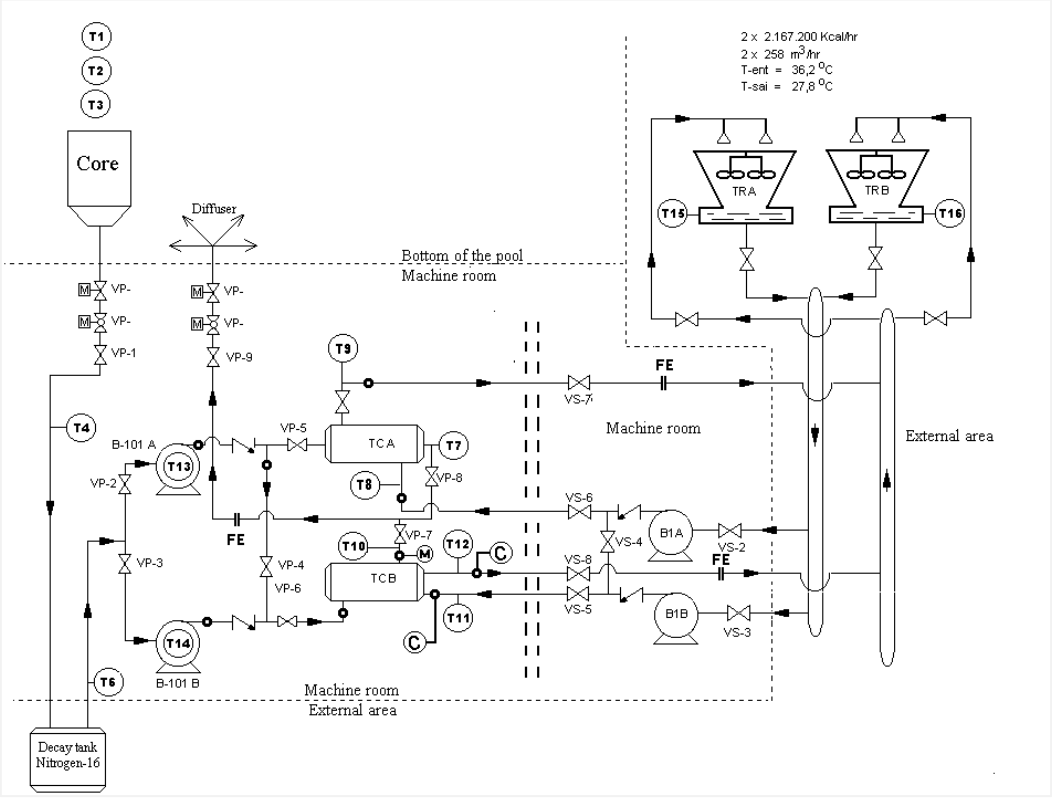

Source: BUENO (2011).

Figure 1 showcases the primary and secondary loops of the reactor, and some of its main components. In the primary loop, water heated by the core flows into the decay tank. From there, it is directed through one of the heat exchangers (TCA or TCB) before being returned to the reactor pool. The secondary loop circulates water between the heat exchanger

and one of the cooling towers (TRA or TRB). Under 200 kW, natural convection is sufficient to cool the reactor (TERREMOTO, 2021). Above that, forced circulation is necessary. Only one set of pumps, heat exchanger and cooling tower is active at any given time, while the other serves as backup.

A Data Acquisition System (DAS) collects two readings per minute of 58 variables (RICCI FILHO and SURKOV, 2007), comprising rod positions, power level, water flow and conductivity, radiation and temperature readings, as listed in Appendix A. The reactor previously operated under a continuous regime for three days a week, at 4.5MW. Currently, it runs for 8h per day, three days a week.

1.2. Objectives

This study aims to expand on previous work by evaluating the performance of FFNNs trained with IEA-R1 data. Specifically, it seeks to assess the networks' generalization ability by testing them across multiple operating cycles using Mean Absolute Percentage Error (MAPE) and sensitivity analysis as performance indicators.

2. MATERIALS AND METHODS

The study was structured into three main stages:

1. Data selection and preprocessing;
2. Network training and validation;
3. Accuracy and sensitivity testing.

Operating cycles were selected from the reactor's event logbook and categorized as either training/validation or testing cycles. The training cycle was chosen due to the absence of sensor faults. Testing cycles were selected to include events and sensor anomalies across all the different types of variables registered by the DAS, as well as different operating

regimes. Variables affected by the events were selected for simulation, and additional variables were chosen to conduct sensitivity tests.

Preprocessing consisted of normalization and noise reduction. Variables of the same physical nature were normalized using a common scaling factor due to their shared value ranges. Noise reduction was carried out using the open-source program SciDAVis, using a moving average filter with a window size of fifteen points.

All subsequent procedures were performed in the open source program SCILAB and its neural network module (TAN and DEBRAY, 2020). The training and validation protocol followed the methodology recommended by BUENO (2011), including the use of predefined input variables, topology and training algorithm:

1. Single-hidden-layer networks trained with the Levenberg-Marquardt algorithm;
2. Two randomly sampled subsets of the training cycle used for training;
3. Five networks were trained per subset, each with randomly initialized weights, targeting a Mean Squared Error (MSE) of $1x10^{-5}$ and a maximum of 1,000 iterations;
4. Validation using remaining data from the training cycle;
5. For each target variable, the best-performing network—based on MAPE—was selected. If no network satisfied the performance criteria, parameters were adjusted and training repeated.

Once networks were selected for all the simulated variables, they were applied to the testing cycles. Sensitivity testing was conducted to cross-reference deviations in the networks to pinpoint the faulty sensor. Figure 2 illustrates a hypothetical variable arrangement and their input/output relationships:

Figure 2: Sensor fault propagation model. Red highlight shows error inVariable 4 and through dependent networks (arrows indicate input relationships).

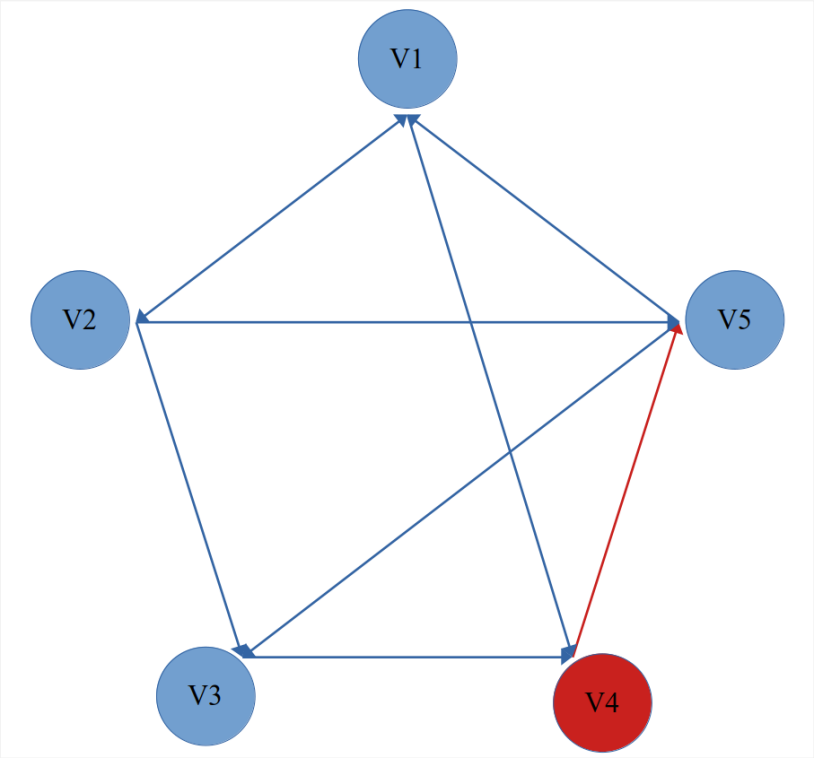

Source: authors.

The diagram represents five variables and the networks that simulate them. Arrows indicate which variables are used as inputs for each network. A fault in Variable Four, highlighted in red, introduces error not only in its corresponding output network but also in the network of Variable Five, as the faulty value propagates through the shared input. Table 1 lists the input-output relationships among the variables:

Table 1: Variable-to-network input relationships (corresponding to Figure 2 topology)

Variable	Input of networks
V1	V2, V4
V2	V1, V3, V5
V3	V4
V4	V5
V5	V1, V3

Source: authors.

Each source of error affects a different set of networks. Therefore, it is possible to pinpoint a faulty sensor based on which networks exhibit deviations. Sensitivity tests, or how changes in the values of one input affect the output of a network, are necessary to assess this method's viability.

Sensitivity tests were conducted by selecting a group of trained networks and systematically introducing a constant offset of 10%, both higher and lower, to a single variable during a test cycle. New outputs were generated, and the MAPE of all networks was recalculated and compared with the original values. For networks where the modified variable served as an input or target, variations in MAPE were expected to exceed the range observed in the training, validation, and test cycles using accurate sensor data.

3. RESULTS AND DISCUSSIONS

Table 2 presents the operating cycles selected for training and testing based on the reactor's event logbook:

Table 2: Reactor operating cycles selected for ANN training and evaluation

Cycle Index	Events listed	Description
Training cycle	None	Continuous operation spanning three days (64 hours total)
01	SCRAM event on day 1; rise in temperature T4 due to loss of flow in secondary circuit on day 2	
02	Unexpected decrease in power on the day 1	
03	SCRAM on the day 3	
04	Reading errors in Z4 safety rod position	8 hours of operation per day, for four days in a week
05		

Source: authors.

Based on the reported events, variables T4, Z4 and N6 were chosen for simulation. To complement sensitivity tests for T4, T1 and T2 were added. Radiation variables MA8 and MD1 and were chosen to complete the selection.

3.1. Training and Validation Performance

In this stage, five of the eight variables were accurately simulated using the original network configurations recommended by BUENO (2011). The remaining three required adjustments in input variables and network structure. Table 3 summarizes the configurations and validation results:

Table 3: Network architectures and validation MAPE ranges

Variable	Initial Network configuration	Final network configuration	Range of MAPE values of the validation process
T1	N3; T2; T6 for inputs. One hidden layer with 05 nodes.	T2; T6 for inputs. One hidden layer with 10 nodes.	Between 4,48% and 7,21%.
T2	T1; T4 for inputs. One hidden layer with 09 nodes.	Initial configuration successful.	Between 0,91% and 1,84%.
T4	T1; T6 for inputs. One hidden layer with 10 nodes.	Initial configuration successful.	Between 0,33% and 0,54%
Z4	Z1; Z3 for inputs. One hidden layer with 10 nodes. Failed training.	N8; Z1; Z3 for inputs. One hidden layer with 10 nodes.	Between 29,96% and 126,96%.
N6	Z1; N7 for inputs. One hidden layer with 10 nodes. Failed training.	Z2; N8 for inputs. One hidden layer with 10 nodes.	Between 0,46% and 0,48%.
MA8	Z1; Z2; MA1; MA2; MD2 for inputs. One hidden layer with 10 nodes.	Initial configuration successful in training.	Between 4,44% and 6,43%.
MD1	MD2; MD3 for inputs. One hidden layer with 08 nodes.	Initial configuration successful.	Between 4,45% and 5,67%.

Source: authors.

Per Table 3, some networks required changes in the input variables to improve performance. In the case of T1, the N3 variable introduced excessive noise and was excluded, with the number of hidden nodes increased to ten. After these modifications, all networks achieved satisfactory performance in the training cycle. Figure 3 shows the percentage error for the Z4 network with the best performance:

Figure 3: Percentage error of the Z4 network during the training and validation cycle

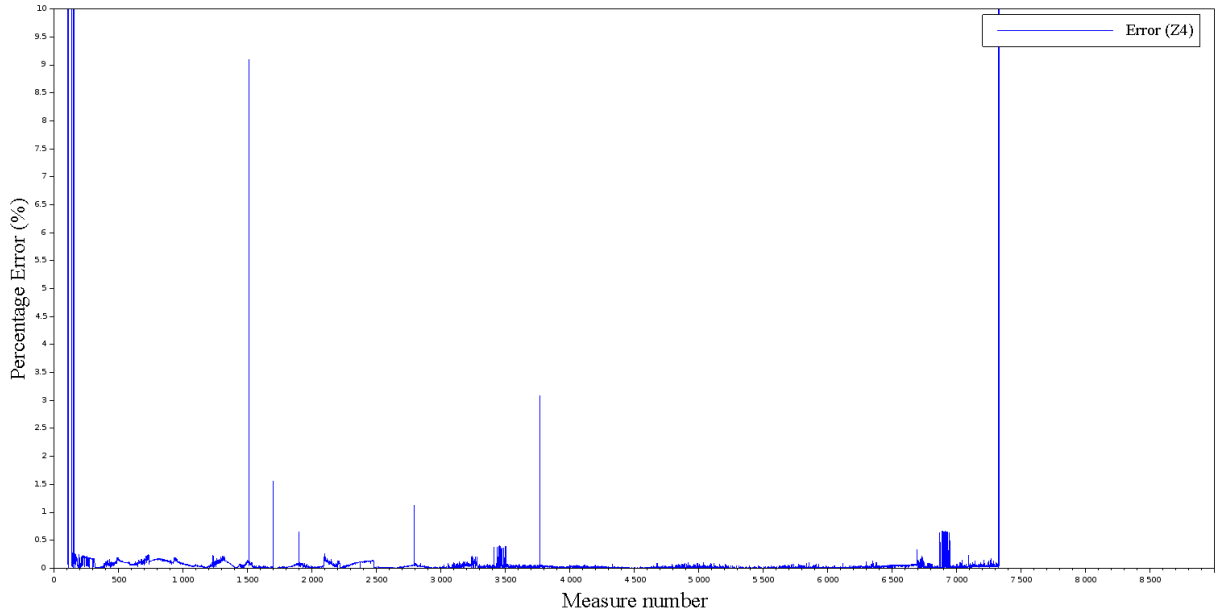

Source: authors.

The Percentage Error of the Z4 network was below 1% for the majority of the training cycle. The high MAPE values stemmed from the differences between sensor and network at the beginning and end of the cycle, when the rod is fully lowered, i.e., it's position goes down to zero. The chosen network was, therefore, the one which followed rod movements the better, instead of the one with the smallest MAPE value.

3.2. Performance in test cycles

Not all networks maintained accuracy during testing. SCRAMs and power maneuvering, including as reactor start-ups and shutdowns, affected all networks. Table 4 summarizes the results of the networks that achieved the best performance in the training cycle:

Table 4: Test cycle summary and performance metrics (MAPE)

Variable	Test summary	Final MAPE values in the test cycles	Mean Performance Ratio: mean $(\sum_i \frac{MAPE\_test_i}{MAPE\_training})$
T1	Initial networks showed poor correlation with sensor curves. The final network successfully tracked sensor readings. SCRAMs and power maneuvering decreased performance.	Between 1,09% and 3,3%.	0.42
T2	Partial overlap was observed between sensor and network outputs. SCRAMs and power maneuvering affected performance.	Between 0,81% and 2,6%.	1.65
T4	Near-complete overlap occurred between sensor and network values, except during power maneuvering.	Between 0,27% and 0,63%.	1.29
Z4	Accurate performance in general, with high percent differences when Z4 reached positions near zero value. Instances where networks failed to track some rod movements.	Between 54,39% and 785,98%.	2.49
N6	High accuracy in cycle 01. Other cycles showed persistent offsets. A sensor scale modification was identified as the cause of systematic offsets. High percentage difference due to periods when the reactor was off.	Between 30,1% and 200,22%.	308.83
MA8	Poor performance, not tracking sensor curves and with high deviations. Highest deviations in SCRAMs and power maneuvering.	Between 186,01% and 12330,45%.	614.56
MD1	The network tracked sensor curves, albeit with consistent offsets in all cycles except Cycle 03.	Between 5,25% and 17,38%.	2.51

Source: authors.

Performance varied between variables and operating conditions. The T4 network performed the best, accurately replicating the temperature rise observed in cycle 01. Figure 4 shows a detailed temporal profile of this event:

Figure 4: Zoomed view of T4 temperature values around the reported rise in test cycle 01

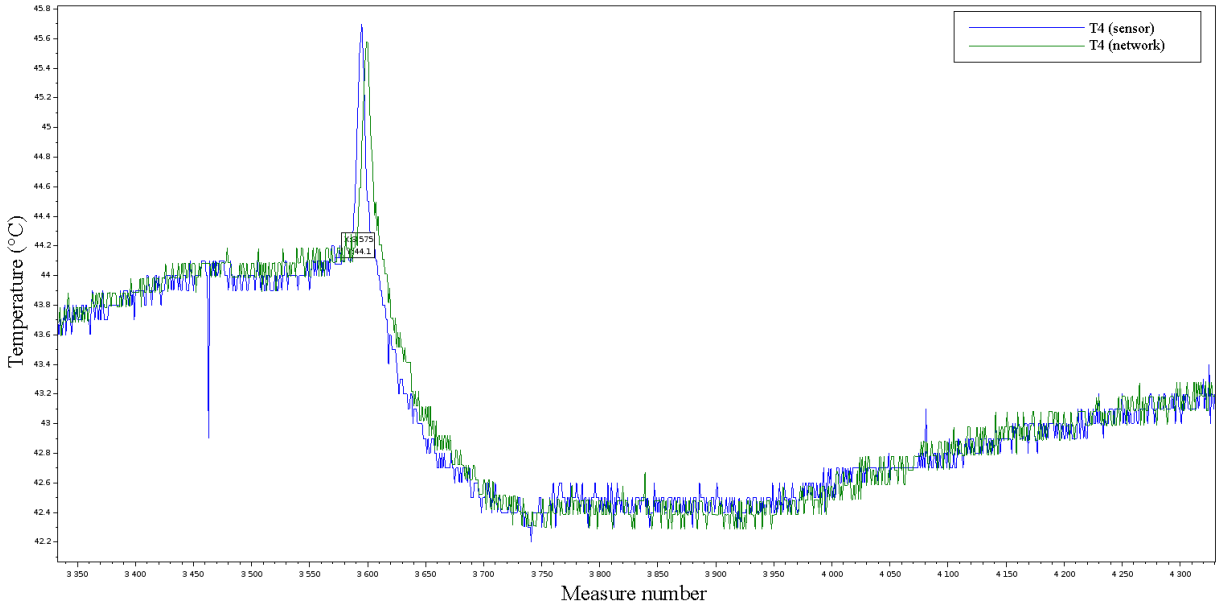

Source: authors.

Albeit with a small time delay, the network closely tracked the sensor's readings. The overlap between sensor and network is present in all T4 curves, with the exception of power maneuvering. T2 showed similar behavior, while T1's performance was slightly lower. Figure 5 illustrates the T1 results for cycle 01:

Figure 5: T1 sensor and network comparison for test cycle 01

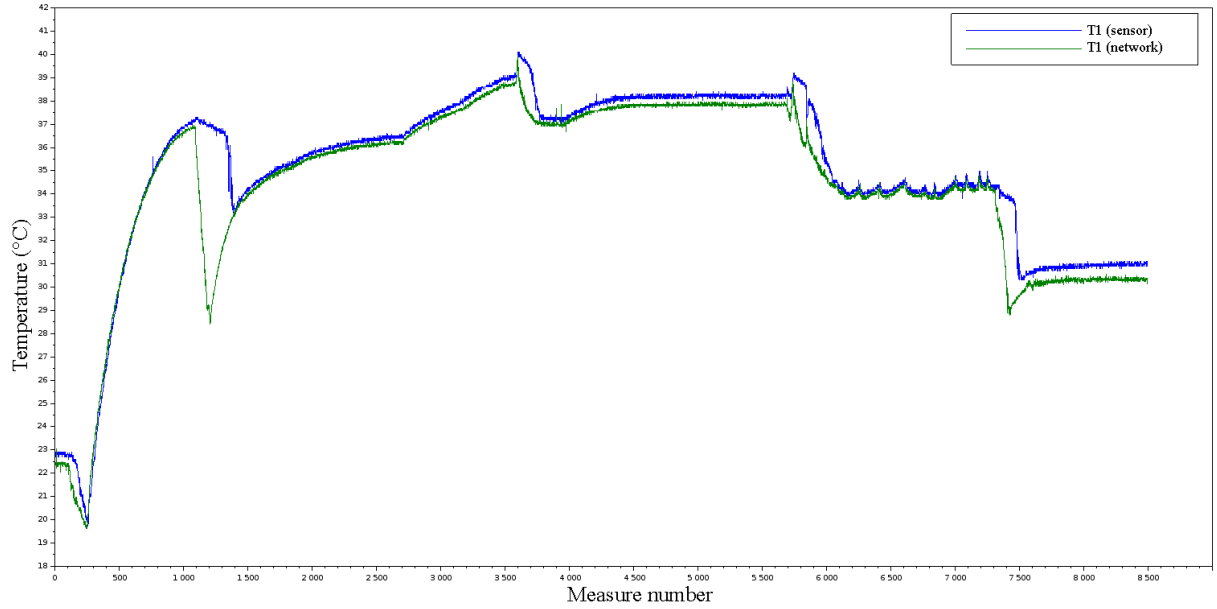

Source: authors.

Larger deviations occurred at the beginning, end, and during the SCRAM event (around time point 1000). While the network tracked the general shape of the signal, its overlap was not as precise as with T2 and T4.

The networks of variables Z4, N6 and MD1 had mixed performance. Figure 6 shows Z4 in cycle 04:

Figure 6: Z4 sensor and network in test cycle 04

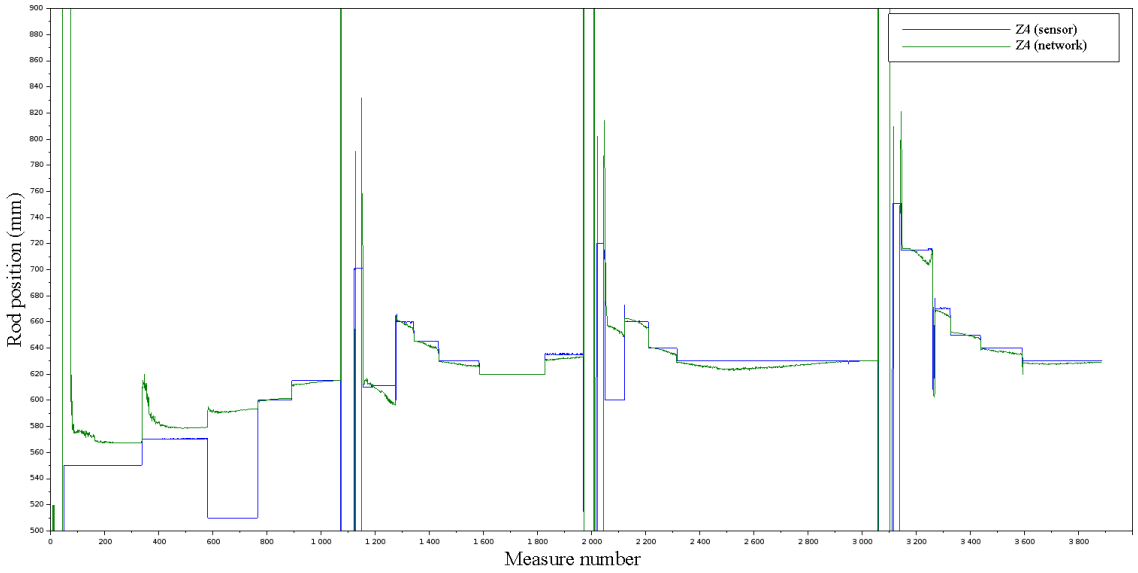

Source: authors.

The rod exhibited stepwise movements—upward or downward. Star-ups and shutdowns occured at time points 0, between 1000 and 1200, around 2000 and between 3000 and 3200. Although the network captured most movements, at certain points (e.g., around time point 600), it moved contrary to the actual rod behavior. As in training, rod positions near zero generated high MAPE values.

In the case of N6, a change in sensor scale between cycles 01 and 02 led to consistent offsets, as illustrated in Figure 7.

Figure 7: N6 sensor and network curves in test cycle 02

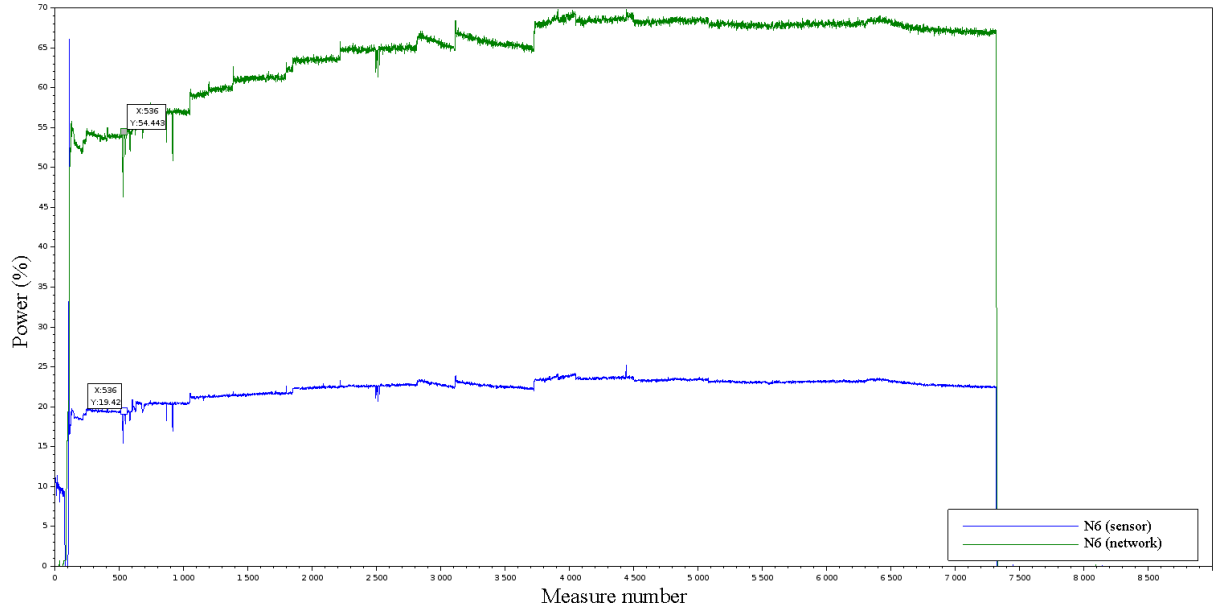

Source: authors.

The highlighted point at time point 536 identifies the reported decrease in power. As reported in Table 4, the network tracks power fluctuations, but with an offset. A similar issue was observed in the case of MD1, as seen in Figure 8:

Figure 8: MD1 sensor and network curves in test cycle 05

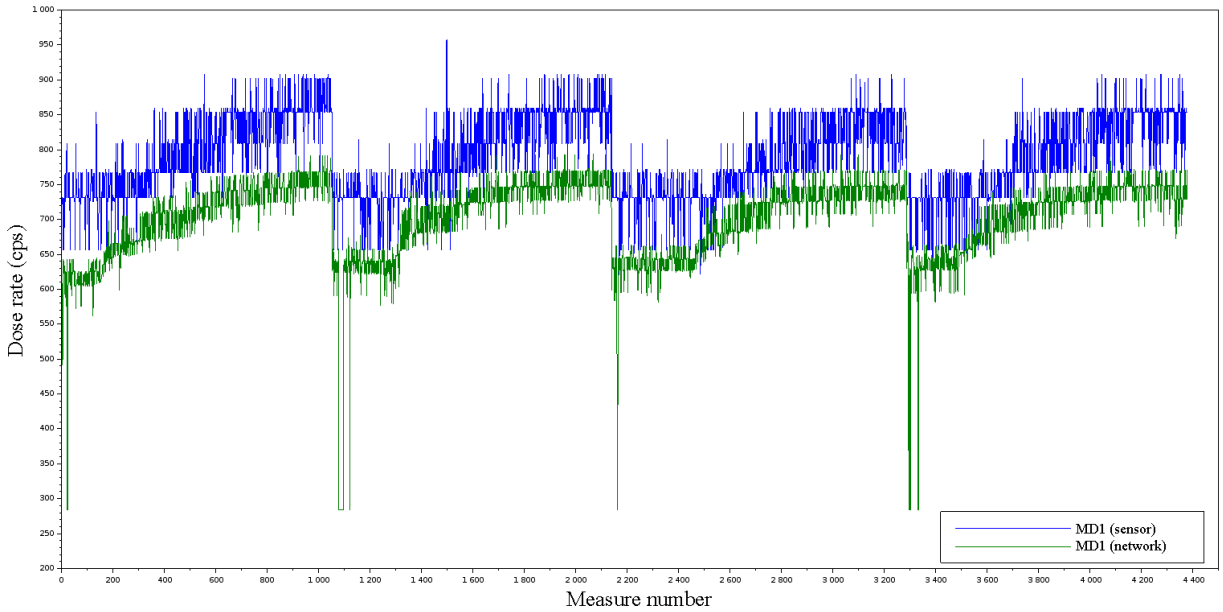

Source: authors.

Unlike N6, no sensor calibration change was reported for MD1. Interestingly, the network performed well in cycle 03, but displayed consistent offsets in other test cycles. In contrast, MA8 networks failed to replicate sensor behavior altogether, as seen in Figure 9:

Figure 9: MA8 sensor and network curves in test cycle 05

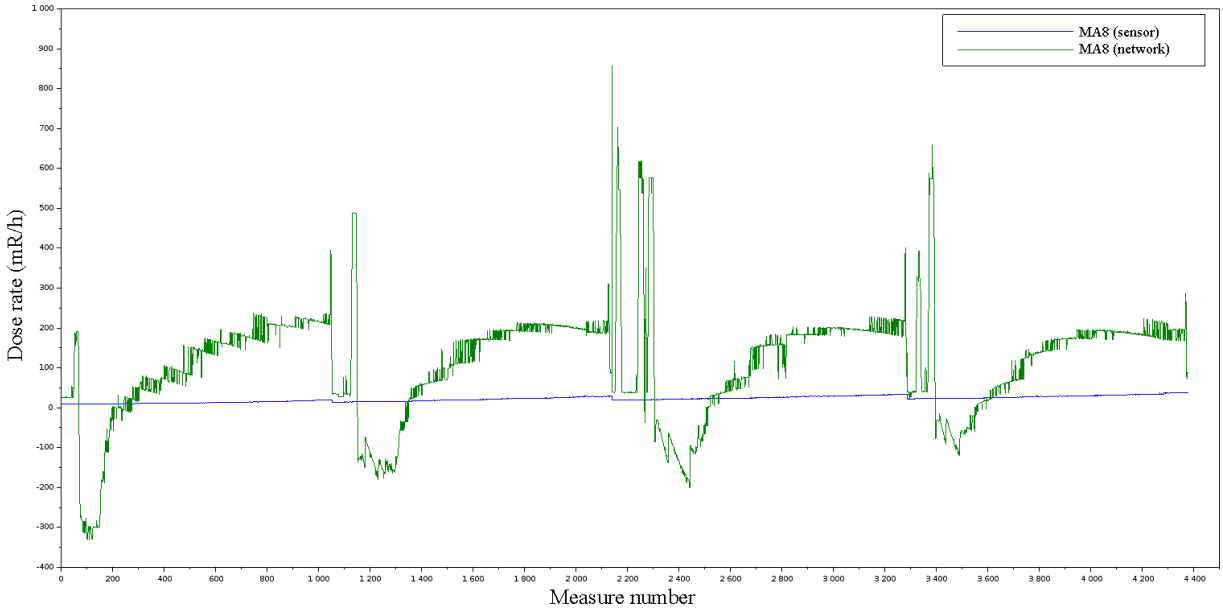

Source: authors.

The network outputs deviated by an order of magnitude, failing to match the shape of the measured signals.

3.3. Sensitivity tests

Variables—T1, T2, and T4—were selected for sensitivity analysis, as their networks demonstrated reliable performance. T6 was also included due to its role as an input variable in some of the networks. Table 5 presents the results of applying constant offsets to selected variables and observing the impact on related networks during test cycle 03.

Table 5: Network output sensitivity to input perturbations (Cycle 03).

Variable	Input of networks	Affected networks (MAPE value)		Unaffected networks (MAPE value)	
		+10%	-10%	+10%	-10%
T1	T2, T4	T2 (3.78%)	T2 (4.86%)	T4 (0.45%)	T4 (0.56%)
T2	T1	T1 (8.12%)	T1 (10.26%)	-	-
T4	T2	T2 (5.77%)	T2 (6.9%)	-	-
T6	T1, T4	T4 (9.8%)	T4 (9.8%)	T1 (1.84%)	T1 (2.86%)

Source: authors.

Per Table 5, offsets introduced in T1 had no discernable effect in the output of the T4 network, as was the case of offsets in T6 and the T1 network. In these cases, MAPE values were within ranges listed in Tables 3 and 4. These results indicate that deviations in either T1 or T2 produce overlapping effects on the same set of networks, which undermines the cross-referencing strategy intended to isolate the faulty sensor.

4. CONCLUSIONS

The performance discrepancy between training/validation and test cycles reveals three key limitations. First, the strong correlation between specific variables (particularly T4 and T6 temperatures) as demonstrated in the sensitivity tests. Statistical methods inherently map these correlations, resulting in a situation where one sensor merely duplicates another, which undermines the goal to achieve redundancy. This corroborates the results regarding Feature Detection of CAIXETA *et al.* (2025).

Second, the single-cycle training data fails to capture operational variations, without incorporating first-principles reactor physics. Networks trained on limited data may capture relationships valid only under specific operational conditions, and fail to generalize across cycles with different dynamics or anomalies. Third, network performance was hampered during power maneuvering. This indicates the need of specialized methodology to categorize data from different operating conditions.

These results demonstrate the necessity of hybrid physics-informed machine learning in future work to improve both model robustness and interpretability.

ACKNOWLEDGMENTS

We thank the staff of the Nuclear and Energy Research Institute (IPEN) for providing access to reactor data and technical support throughout the research process.

FUNDING

This research was financed by the Coordination for the Improvement of Higher Education Personnel (CAPES Foundation), through the CAPES/PROEX 88887.752987/2022-00.

CONFLICTS OF INTEREST

All authors declare no competing interests.

DATA AVAILABILITY STATEMENT

The authors declare that the data supporting the results of this study are available in the article. Derived data supporting the conclusions of this study are available upon request from the corresponding author.

REFERENCES

[1] BARTLETT, E. B.; UHRIG, R. E. Nuclear power plant status diagnostics using an artificial neural network. **Nuclear Technology**, v. 97, n. 3, p. 272–281, 1992.

[2] BUENO, E. I. **Group Method of Data Handling (GMDH) e Redes Neurais na Monitoração e Detecção de Falhas em Sensores de Centrais Nucleares**. 2011. Tese (Doutorado em Tecnologia Nuclear - Reatores) — Instituto de Pesquisas Energéticas e Nucleares, Universidade de São Paulo, São Paulo, 2011. Disponível em: https://doi.org/10.11606/T.85.2011.tde-02092011-140535. Acesso em: 19 out. 2021.

[3] CAIXETA, B. M. et al. Optimizing Deep Neural Networks for Nuclear Power Plant Temperature Estimation: A Study on Feature Importance and Outlier Detection. **SSRN Electronic Journal**, [S.I.]. 2025. Disponível em: https://papers.ssrn.com/sol3/papers.cfm?abstract_id=5131784. Acesso em: 03 nov. 2025.

[4] DENG, A.; HOOI, B. Graph neural network-based anomaly detection in multivariate time series. **Proceedings of the AAAI Conference on Artificial Intelligence**, v. 35, n. 5, p. 4027–4035, 2021.

[5] GOMES, C. R.; MEDEIROS, J. A. C. C. Neural network of Gaussian radial basis functions applied to the problem of identification of nuclear accidents in a PWR nuclear power plant. **Annals of Nuclear Energy**, v. 77, p. 285–293, 2015.

[6] LEE, G.; LEE, S. J.; LEE, C. A convolutional neural network model for abnormality diagnosis in a nuclear power plant. **Applied Soft Computing**, v. 99, p. 106874, 2021.

[7] MANDAL, S. Sensor fault detection in nuclear power plant using artificial neural network. **Journal of Mathematics and Informatics**, v. 4, p. 81–87, 2015.

[8] MESSAI, A. et al. On-line fault detection of a fuel rod temperature measurement sensor in a nuclear reactor core using ANNs. **Progress in Nuclear Energy**, v. 79, p. 8–21, 2015.

[9] MORAES, D. A. **Planta experimental para monitoração e diagnóstico de falhas utilizando inteligência artificial**. 2019. Tese (Doutorado em Tecnologia Nuclear - Reatores) - Instituto de Pesquisas Energéticas e Nucleares, Universidade de São Paulo, São Paulo, 2019. Disponível em: https://doi.org/10.11606/T.85.2020.tde-03022020-110813. Acesso em: 27 jul. 2025.

[10] NABESHIMA, K. et al. Real-time nuclear power plant monitoring with neural network. **Journal of Nuclear Science and Technology**, v. 35, n. 2, p. 93–100, 1998.

[11] NABESHIMA, K. et al. Nuclear reactor monitoring with the combination of neural network and expert system. **Mathematics and Computers in Simulation**, v. 60, n. 3–5, p. 233–244, 2002.

[12] RICCI FILHO, W.; SURKOV, V. **Sistema de Aquisição de Dados do Reator IEA-R1 – SAD – Lista de Variáveis**. São Paulo: Instituto de Pesquisas Energéticas e Nucleares, 2007. Não publicado.

[13] SAEED, A.; RASHID, A. Development of core monitoring system for a nuclear power plant using artificial neural network technique. **Annals of Nuclear Energy**, v. 144, p. 107513, 2020.

[14] SANTOS, G. R. dos. **Algoritmo de Colônia de Formigas e Redes Neurais Artificiais Aplicados na Monitoração e Detecção de Falhas em Centrais Nucleares**. 2016. Dissertação (Mestrado em Tecnologia Nuclear) — Instituto de Pesquisas Energéticas e Nucleares, Universidade de São Paulo, São Paulo, 2016. Disponível em: https://doi.org/10.11606/D.85.2016.tde-02082016-144618. Acesso em: 16 jan. 2024.

[15] TAN, C. L.; DEBRAY, Y. Neural Network Module, v. 3.0. 2020. Disponível em: https://atoms.scilab.org/toolboxes/neuralnetwork/3.0. Acesso em: 24 out. 2024.

[16] TERREMOTO, L. A. A. **Fundamentos de Tecnologia Nuclear – Reatores**. São Paulo: Instituto de Pesquisas Energéticas e Nucleares, Divisão de Ensino, 2021.

[17] YUE, Q. et al. Method to determine nuclear accident release category via environmental monitoring data based on a neural network. **Nuclear Engineering and Design**, v. 367, p. 110789, 2020.

APPENDIX A

List of variables from the IEA-R1 Data Acquisition System (DAS), all sampled at 0.5 Hz, used in the research.

Table 6: IEA-R1 variables monitored by the Data Acquisition System (DAS).

Category	Variable Code	Parameter description	Unit of measurement
NUCLEAR	Z1	Control rod position	[mm]
	Z2	Safety rod 1 position	[mm]
	Z3	Safety rod 2 position	[mm]
	Z4	Safety rod 3 position	[mm]

Category	Variable Code	Parameter description	Unit of measurement
	N3	Power (safety channel 2)	[%]
	N6	Power (linear channel)	[%]
	N7	Demand percentage	[%]
	N8	Power (channel N16)	[%]
RADIATION	MA1	Dose rate – core support bridge, left	[mR·h^{-1}]
	MA2	Dose rate – core support bridge, right	[mR·h^{-1}]
	MA8	Dose rate – water treatment system (resin column)	[mR·h^{-1}]
	MD1	Dose rate – 1st-floor air exhaust duct	[cps]
	MD2	Dose rate – 3rd-floor air exhaust duct	[cps]
	MD3	Dose rate – general exhaust duct, 4th floor	[cps]
TEMPERATURE	T1	Pool surface temperature	[°C]
	T2	Mid-pool water temperature	[°C]
	T4	Decay tank inlet temperature	[°C]
	T6	Decay tank outlet temperature	[°C]

LICENSE